partitioned among the products' vibrational modes; i.e., the full reaction exoergicity is not available for vibrational excitation of the fragments. Thus, as the transition state is transformed to products, the fragments are vibrationally decoupled from one another. The potential energy associated with the activation barrier is channeled principally to the relative translational motion of the products.

Acknowledgement is made to the donors of the Petroleum Research Fund, administered by the American Chemical Society, for partial support of this work. In addition, support for this work was provided by a grant from the National Science Foundation (NSF CHE-8206897).

Registry No. 3-Cyclopentenone, 14320-37-7.

Kinetics of Polyatomic Free Radicals Produced by Laser Photolysis. 3. Reaction of Vinyl Radicals with Molecular Oxygen

Irene R. Slagle, Jong-Yoon Park, Michael C. Heaven, and David Gutman*

Contribution from the Department of Chemistry, Illinois Institute of Technology, Chicago, Illinois 60616. *Received December 19, 1983*

Abstract: The kinetics and mechanism of the gaseous reaction of vinyl radicals with molecular oxygen have been studied between 297 and 602 K. The radicals were produced in a heated tubular reactor by the pulsed laser photolysis of C_2H_3Br at 193 nm. Reactant and product concentrations were monitored in real-time experiments using photoionization mass spectrometry. The products formed in this temperature range are HCO and H_2CO. The overall rate constant is pressure independent and is nearly constant with temperature: $k = 6.6\ (\pm 1.3) \times 10^{-12} \exp(250 \pm 100\ \text{cal}/RT)\ \text{cm}^3\ \text{molecule}^{-1}\ \text{s}^{-1}$. The magnitude of the rate constant, its temperature and pressure dependence, and the identity of the products of this reaction indicate that it proceeds by an addition mechanism in which the adduct rapidly rearranges to form an energy-rich dioxetanyl intermediate which decomposes into the observed products. Two other reactions (C_2H_3 + i-C_4H_{10} and C_3H_5 (allyl radical) + O_2) were investigated at elevated temperatures, but no reaction was detected. An upper limit (5×10^{-14} cm^3 molecule^{-1} s^{-1}) was established for the rate constants of both C_2H_3 + i-C_4H_{10} at 600 K and C_3H_5 + O_2 at 900 K.

Unsaturated hydrocarbon free radicals such as alkenyl and alkynyl radicals are particularly important intermediates in combustion processes.[1-3] These energy-rich hydrogen-deficient reaction intermediates are formed by the reactions of alkenes and alkynes with atoms and free radicals (such as H and OH),[4-6] and they subsequently react in two fundamentally different ways. They may react with molecular oxygen in extremely exothermic reactions that lead to stable oxygen-containing products or they may continue to lose hydrogen atoms in endothermic pyrolysis reactions that ultimately result in the production of soot precursors such as C_2H and C_3H_2.[5-9] A complete understanding of the kinetics and mechanisms of these two competing processes is essential for the quantitative modeling of macroscopic combustion phenomena such as soot formation and for the prediction of stable product yields.

A considerable amount of information is available on the thermal decomposition of free radicals based on experimental studies,[7,10-14] on additional investigations of the reverse reactions and the appropriate equilibrium constants,[15] and on estimates based on theoretical and thermochemical considerations.[16,17] Virtually nothing is known about the mechanisms or the rates of the reactions of unsaturated hydrocarbon free radicals with molecular oxygen. Only one has ever been isolated for direct study (C_2H + O_2),[18,19] and there is only one report of an indirect investigation of their mechanisms.[4] We have begun a series of studies of the reactions of unsaturated free radicals that are important in combustion processes. The first has involved the kinetics and mechanism of the C_2H_3 + O_2 reaction. This elementary reaction has never been isolated for direct study before, and there is no knowledge of its rate constant parameters. The results of this investigation are reported here.

Current kinetic models of combustion processes presume that the mechanism of the vinyl-radical reaction with O_2 at high temperatures is[5,7,9]

$$C_2H_3 + O_2 \rightarrow C_2H_2 + HO_2 \qquad \Delta H = -7\ \text{kcal} \qquad (1)$$

The use of this mechanism is based on the presumption that the C_2H_3 + O_2 reaction proceeds analogously to the C_2H_5 + O_2 reaction,[20] which is known to proceed by H-atom transfer to O_2

(1) Pollard, R. T. In "Comprehensive Chemical Kinetics"; Bamford, C. H., Tipper, C. F. H., Eds.; Elsevier: New York, 1977; Vol. 17, Chapter 2.
(2) Gardiner, W. C., Jr. *Sci. Am.* **1982**, *246*, 110.
(3) Warnatz, J.; Bockhorn, H.; Moser, A.; Wenz, H. W. *Symp. (Int.) Combust. [Proc.]* **1983**, *19*, 197-209.
(4) Baldwin, R. R.; Walker, R. W. *Symp. (Int.) Combust. [Proc.]* **1981**, *18*, 819-829.
(5) Westbrook, C. K.; Dryer, F. L.; Schug, K. P. *Combust. Flame* **1983**, *52*, 299-313.
(6) Homann, K. H.; Wellmann, Ch. *Ber. Bunsenges. Phys. Chem.* **1983**, *87*, 609-616.
(7) Warnatz, J. Report SAND83-8606; Sandia: Livermore, CA, Feb 1983.
(8) Westbrook, C. K.; Dryer, F. L. Report UCRL-88651; Lawrence Livermore National Laboratory: Livermore, CA, Feb 1983.
(9) Miller, J. A.; Mitchell, R. E.; Smooke, M. D.; Kee, R. J. *Symp. (Int.) Combust. [Proc.]* **1983**, *19*, 181-196.
(10) Walker, R. W. In "Gas Kinetics and Energy Transfer"; Ashmore, P. G., Donovan, R. J., Eds.; Chemical Society: London, 1977; Vol. 2, Chapter 7.
(11) Jachimowski, C. *J. Combust. Flame* **1977**, *29*, 55.
(12) Roth, P.; Barner, U.; Lohr, R. *Ber. Bunsenges. Phys. Chem.* **1979**, *83*, 929-932.
(13) Benson, S. W.; Haugen, G. R. *J. Phys. Chem.* **1967**, *71*, 1735-1746.
(14) Leathard, D. A.; Purnell, J. H. *Ann. Rev. Phys. Chem.* **1970**, *21*, 197.
(15) Payne, W. A.; Stief, L. J. *J. Chem. Phys.* **1976**, *64*, 1150.
(16) Choo, K. Y.; Benson, S. W. *Int. J. Chem. Kinet.* **1981**, *13*, 833.
(17) Burcat, A.; Skinner, G. B.; Grossley, R. W.; Scheller, K. *Int. J. Chem. Kinet.* **1973**, *5*, 345.
(18) Lange, W.; Wagner, H. Gg. *Ber. Bunsenges. Phys. Chem.* **1975**, *79*, 165-170.
(19) Laufer, A. H.; Lechleider, R. *J. Phys. Chem.* **1984**, *88*, 66-68.

0002-7863/84/1506-4356$01.50/0

at elevated temperatures.[21,22] The rate constants used for reaction 1 in combustion models are derived from an Arrhenius expression for k_1 suggested by Cooke and Williams in their study of ignition delays in shock-heated ethane–oxygen mixtures ($k_1 = 2.6 \times 10^{-11}$ exp(−10 kcal/RT) cm^3 molecule^{-1} s^{-1}).[20] The measured induction times in this study were modeled with a 34-step mechanism that included reaction 1. The rate constant of this as well as other reactions was varied to obtain a reasonable fit of the measurements to the model. The suggested 10-kcal activation energy is due primarily to the belief at the time of the study that reaction 1 is 8–9 kcal endothermic (current thermochemical information indicates that it is actually about 7 kcal exothermic).[23]

Baldwin and Walker have studied the mechanism of the $C_2H_3 + O_2$ reaction at 480 °C.[4] The study involved the addition of C_2H_4 to slowly reacting mixtures of $H_2 + O_2$ and the determination of the identity and yield of the stable products produced. The vinyl radicals were produced by abstraction reactions involving C_2H_4 and H or OH, intermediates generated by the $H_2 + O_2$ reaction. No trace of C_2H_2 was detected, which was cited as evidence that reaction 1 is not the correct mechanism for the $C_2H_3 + O_2$ reaction. In this study, the major carbon-containing end products that were detected and that could not be attributed to addition reactions involving C_2H_4 were CO and H_2CO. This led to the conclusion that the $C_2H_3 + O_2$ reaction proceeds by the highly exothermic route

$$C_2H_3 + O_2 \rightarrow HCO + H_2CO \qquad \Delta H = -80 \text{ kcal} \quad (2)$$

In our investigation of the $C_2H_3 + O_2$ reaction, we have conducted a search for the possible initial products using time-resolved photoionization mass spectrometry in order to directly identify its reactive routes. We have also measured the overall rate constant as a function of temperature to obtain the Arrhenius parameters and as a function of pressure to obtain information on the reaction mechanism.[25]

Experimental Apparatus

The apparatus and most procedures used were essentially the same as those described in parts 1 and 2.[26,27] The experiments were performed by using a tubular reactor coupled to a photoionization mass spectrometer (PIMS) detector. Gas flowing through the reactor was irradiated with almost uniform intensity along the reactor's length with a UV photolysis laser. In the experiments performed to study the kinetics and mechanism of the $C_2H_3 + O_2$ reaction, the gas flowing through the reactor contained the C_2H_3 soure (0.002–0.01% C_2H_3Br), varying amounts of O_2 (0.02–0.30%), and a large excess of He buffer gas (≈99%). The total gas densities used varied from 1–6 × 10^{16} molecule cm^{-3}.

Gas was continuously sampled from a 0.044-cm-diameter hole in the side of the reactor. The emerging gas was formed into a beam by a conical skimmer as it entered the vacuum chamber containing the PIMS. As the gas traversed the ion source, a portion was photoionized and mass selected. The distance from the sampling orifice in the reactor to the center of the ionizing region of the PIMS was 2.4 cm.

Temporal ion signal profiles of reactants and possible products were recorded with a multichannel scalar from a period just before each laser pulse to up to 50 ms following the pulse.

Intense atomic resonance lamps were used to provide the photoionizing radiation in the PIMS. In each experiment a lamp was used that has a resonance radiation energy just above that needed to ionize the species of interest. In these studies the Ar lamp (11.8 eV) was used to detect HBr, Br, C_2H_2, and H_2CO, the H lamp (10.2 eV) to detect C_2H_3Br, C_2H_3, and HCO, and the Cl lamp (8.9 eV) to detect C_3H_5.

I. Generation of Vinyl Radicals. Two major changes were made in the apparatus for these experiments. The first involved the use of laser photolysis of C_2H_3Br at 193 nm as a pulsed source of vinyl radicals. The unfocused output of a Lumonics TE-861-4 excimer laser operated with ArF was attenuated with a wire screen (to ca. one-third the original intensity) and then directed along the axis of the 0.95-cm i.d. tubular Pyrex flow reactor which has a quartz window at one end and a beam stop and pumping port at the other. The laser output was collimated with an iris into a slowly diverging beam that filled the reactor. Typically the laser was operated at 11 Hz at a pulse energy of 20–30 mJ. Under these conditions 10–15% of the C_2H_3Br decomposed during each laser pulse. A rapid gas flow velocity, ≈10 m/s, assured that the photolyzed gas was replaced between laser pulses.

The reactor walls were coated with boric acid after washing with a 5% NH_4F·HF solution. The condition of the walls deteriorated slowly during these experiments (as manifested by an apparent wall-decay rate constant for the vinyl radicals that slowly increased). The wall of the tubular reactor could, however, be restored to its original condition by passing an oxygen atom containing flow through it for 30 min. This was done as needed, usually at the end of each day's experiments.

In these studies, the initial concentration of C_2H_3 was kept low (≈10^{11} molecules cm^{-3}) to ensure that reactions between reaction intermediates had negligible rates compared to that of the $C_2H_3 + O_2$ reaction.

II. Construction and Performance of the Heatable Reactor. The second major change in the experimental apparatus involved the use of a heater tubular reactor. The flow tube was tightly wrapped with a nichrome ribbon (1.0 cm wide, 0.0003 cm thick) in a spiral that extended from 19.5 cm upstream to 7.5 cm downstream from the sampling orifice. The space between turnings was less than 1 mm. A small hole was cut in the turning that covered the gas-sampling orifice to permit unimpeded gas flow from the reactor. No thermal shielding was used. The reactor was heated by passing an alternating current provided by a Variac autotransformer through the ribbon heater. Operation at temperatures up to 900 K was routine. The reactor has been used up to 1000 K. A quartz tube was used instead of the Pyrex one for those experiments conducted above 700 K. Little power was needed to maintain high temperatures, 35 W at 600 K and 210 W at 900 K.

Measurements were made to determine the temperature uniformity along the tubular flow reactor. These tests were conducted over the full range of densities, temperatures, and flow velocities used in these studies. The carrier gas was He in all cases. Temperatures were measured with a thermocouple that could be moved along the axis of the reactor. The results of these tests established that the uniformly heated zone in the reactor extends from 15 cm upstream from the gas-sampling point to 3 cm beyond it. Below 200 °C the temperature in this zone has a uniformity better than ±5 °C, and above 300 °C it is better than ±10 °C.

The temperature during an actual experiment is monitored by an in situ thermocouple placed in the heated zone of the reactor. A $^1/_{16}$-in.-diameter, stainless-steel-sheathed chromel–alumel thermocouple was located 3 cm downstream from the sampling orifice. It was held in the center of the flow tube by thin metal supports. The thermocouple leads passed through the beam stop at the downstream end of the reactor. The temperature readings of the in situ thermocouple agreed with those recorded with the movable thermocouple when the latter was placed farther upstream (in the middle of the 15-cm-long zone from which gas was sampled during an experiment). The period during which the reaction under study could be monitored extended from the moment the laser initiates it to the time of arrival at the sampling point of the last gas element from the uniformly heated zone (≈14 ms when the flow velocity is 11 m/s).

There was no increase in temperature recorded on the thermocouple when the laser was turned on.

III. Source and Purification of Gases. C_2H_3Br, i-C_4H_{10} (>99%), and argon (prepurified) were obtained from Matheson and C_3H_5Br from Aldrich. C_2H_3Br and C_2H_2 (obtained from Midwest Welding Co.) were purified by fractional distillation and stored in stainless steel tanks, the former as a dilute mixture (10% in Ar). Helium (high purity) and O_2 (extra dry) were obtained from Linde and were used without extra purification. Argon and C_3H_5Br were also not purified further.

Experimental Results

I. 193-nm Photolysis of Vinyl Bromide. A survey was conducted to determine the products produced by the 193-nm photolysis of C_2H_3Br. Most of these experiments were performed at 599 K (additional ones were conducted at room temperature where similar results were obtained). A gas mixture was flowed through the reactor at a pressure of 3.6 torr that contained C_2H_3Br

(20) Cooke, D. F.; Williams, A. *Symp. (Int.) Combust. [Proc.]* **1971**, *13*, 757–766.

(21) Baldwin, R. R.; Pickering, I. A.; Walker, R. W. *J. Chem. Soc., Faraday Trans. 1*, **1980**, *76*, 2374–2382.

(22) Baldwin, R. R.; Hopkins, D. E.; Walker, R. W. *Trans. Faraday Soc.* **1970**, *66*, 189.

(23) Values of ΔH for reactions 1, 2, and 4 were determined from heats of formation in ref 24 except HO_2 (obtained from: Howard, C. J. *J. Am. Chem. Soc.* **1980**, *102*, 6937–6941) and C_2H_3 (obtained from: Ayranci, G.; Back, M. H. *Int. J. Chem. Kinet.* **1983**, *15*, 83–104). This reference also includes a discussion of the discrepancies that exist among the reported values of the C_2H_3 heat of formation.

(24) Benson, S. W. "Thermochemical Kinetics"; Wiley: New York, 1976.

(25) A preliminary report of this study has been published: Park, J.-Y.; Heaven, M. C.; Gutman, D. *Chem. Phys. Lett.* **1984**, *104*, 469–474.

(26) Slagle, I. R.; Yamada, F.; Gutman, D. *J. Am. Chem. Soc.* **1981**, *103*, 149–153.

(27) Slagle, I. R.; Gutman, D. *J. Am. Chem. Soc.* **1982**, *104*, 4741–4748.

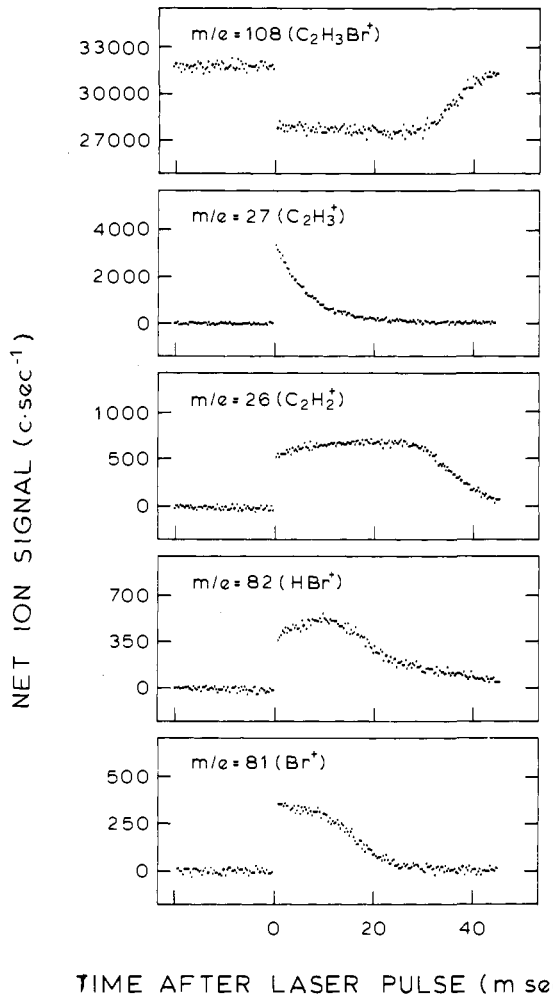

Figure 1. Temporal ion signal profiles of C_2H_3Br and its photolysis products at 193 nm. Experimental conditions: p = 3.61 torr (primarily He), $[C_2H_3Br]$ = 1.8 × 10^{12} molecule cm^{-3}, T = 599 K. Extent of C_2H_3Br photolysis: ≈14%.

(0.003%) and He (balance). Possible products were monitored by using photoionizing energies of 10.2 and 11.8 eV in the mass spectrometer. The only significant products that were detected were C_2H_3, C_2H_2, Br, and HBr. This indicates two important photolysis routes:

$$C_2H_3Br + 193\ nm \xrightarrow{a} C_2H_3 + Br$$
$$\xrightarrow{b} C_2H_2 + HBr \qquad (3)$$

Products that were searched for but were not detected include CH_2, CH_3, and CH_2Br.

The temporal ion signal profiles of the four detected photolysis products as well as that of vinyl bromide are shown in Figure 1. The period covered by these profiles extends from 20 ms before the laser pulse to 50 ms after the pulse and therefore includes ion signals from those gas elements that were in the uniformly heated zone during each pulse (0–14 ms), from gas elements that were in the zone where the temperature returns to room temperature (14–30 ms), and from the gas that was located near the window that admits the laser light (and where the unphotolyzed gas enters the flow tube, 30–50 ms).

The constant magnitude of the depleted C_2H_3Br ion signal for 30 ms of sampling time after the laser pulse indicates that the extent of the photolysis is uniform along the reactor not only in the zone that is heated to 600 K but also throughout the region wherein the temperature is dropping to room temperature. The mixing zone between photolyzed and unphotolyzed gas is very apparent in this profile. The C_2H_3Br depletion can be accurately measured by using these ion signal profiles and used to determine

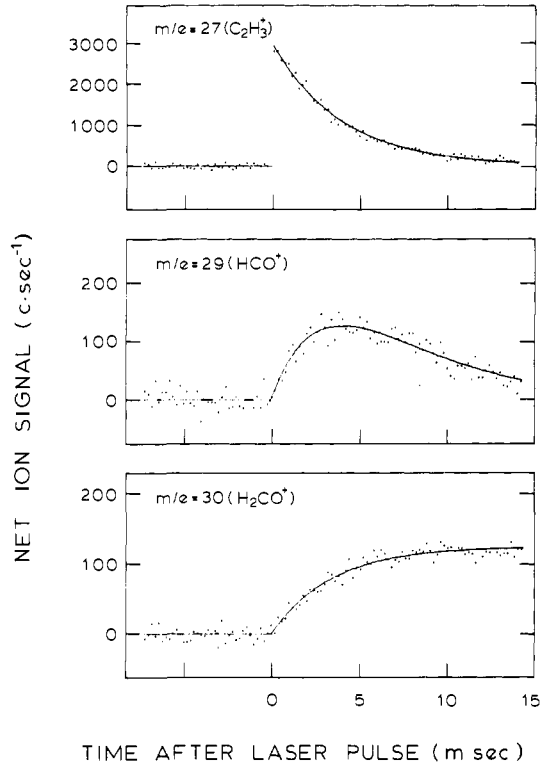

Figure 2. Temporal ion signal profiles of reactant and products of C_2H_3 + O_2 reaction. Experimental conditions: p = 3.61 torr (primarily He), $[C_2H_3Br]$ = 1.79 × 10^{12} molecule·cm^{-3}, $[O_2]$ = 1.42 × 10^{13} molecule·cm^{-3}, T = 599 K.

the fraction of C_2H_3Br decomposed during each laser pulse.

The vinyl radical ion signal decays exponentially. The decay rate constant is very sensitive to the condition of the walls and is relatively insensitive to the vinyl bromide concentration. Radical loss under these experimental conditions is essentially all heterogeneous. Typical first-order wall-loss rate constants were 130 s^{-1} at 600 K and somewhat higher at room temperature (typically 180 s^{-1}).

The reaction undergone by the C_2H_3 radical on the walls of the reactor is suggested by the $C_2H_2^+$ ion signal profile. It rises promptly at t = 0 due to the production of C_2H_2 by the initial photolysis process. It then continues to grow from that time on in an exponential manner with a growth constant that is essentially the same as that observed for the C_2H_3 decay. If O_2 is present in excess (to scavenge the C_2H_3 radicals as they are formed), the $C_2H_2^+$ ion signal profile rises sharply as before at t = 0, but it does not continue to grow. No C_2H_4 or C_2H_6 is observed to appear following laser photolysis in the absence of O_2. These observations taken together suggest that the wall reaction is primarily one involving H-atom loss to form C_2H_2.

Both the Br^+ and HBr^+ ion signals also rise promptly at t = 0. That of Br^+ decays slowly and that of HBr^+ rises significantly during the period that gas is being sampled from the homogeneously heated zone. Both drop almost precipitously during the period that gas from the zone that is not uniformly heated is being sampled. The early behavior is most likely due to the conversion of Br to HBr, possibly by the heterogeneous reaction

$$C_2H_3 + Br \xrightarrow{wall} C_2H_2 + HBr \qquad \Delta H = -45\ kcal \qquad (4)$$

The rapid loss of Br and HBr at longer times (in gas elements outside the uniformly heated zone) is not understood.

The extent of photolysis by reaction 3b was determined at both 298 and 601 K. C_2H_2 formation was compared to C_2H_3Br depletion. Mass spectrometer sensitivities to both molecules were determined by using metered flows of both into the flow reactor. The yield of C_2H_2 during photolysis ($-\Delta[C_2H_2]/\Delta[C_2H_3Br]$) was essentially the same at both temperatures: 0.59 ± 0.05 at 298 K and 0.55 ± 0.05 at 601 K.

II. Products of the $C_2H_3 + O_2$ Reaction. A search was conducted for products of the $C_2H_3 + O_2$ reaction at both room temperature and 599 K. A gas mixture containing C_2H_3Br (0.003%), O_2 (0.02%), and He (balance) was flowed through the reactor, and possible products of this reaction were monitored. The only products detected at both temperatures were HCO and H_2CO. The temporal behavior of the ion signals of these two products and the fact that their ion signals were absent when O_2 was not present indicate that they are products of the $C_2H_3 + O_2$ reaction (see Figure 2). The possible products that were searched for but were not detected (using both 10.2- and 11.8-eV ionizing energies) include CH_3, CH_2Br, HO_2, $C_2H_3O_2$, and C_2H_3O. No C_2H_2 was produced after the original photolysis process at both temperatures. C_2H_2 yields were measured with and without O_2 present and were found to be the same ($<\pm 5\%$). This places an upper limit of 10% on the extent that the $C_2H_3 + O_2$ reaction could be proceeding by reaction 1 between 298 and 599 K.

These experiments identify reaction 2 as a major route of the $C_2H_3 + O_2$ reaction at both ambient temperature and 600 K. A very minor ion signal was also recorded for one additional possible product, C_2H_2O. This signal was too poor to establish its temporal behavior. Our detection method happens to be extremely sensitive for detecting C_2H_2O.[28] We can therefore conclude that an additional possible route, that which produces C_2H_2O and OH, if it indeed does exist, is of very minor importance.

Neither of the two detected product ion signals, HCO^+ or H_2CO^+, could have resulted from the fragmentation of possible products of higher mass. In particular HCO^+, which was detected by using 10.2-eV ionizing energy, could not have been produced by the fragmentation of the formylmethyl radical, CH_2CHO, since this process is 12.4 eV endothermic.[29]

To determine whether the temporal evolution of the measured product ion signal profiles are those expected of initial products of the $C_2H_3 + O_2$ reaction, both $I(HCO^+)$ and $I(H_2CO^+)$ were fitted to analytical expressions that were derived from the presumed kinetic mechanism for this system. The laser photolysis initiated the sequence of reactions listed below:

$$C_2H_3Br + h\nu\ (193\ nm) \rightarrow C_2H_3 + Br \qquad (3a)$$

$$C_2H_3 + O_2 \rightarrow HCO + H_2CO \qquad (2)$$

$$C_2H_3 \rightarrow \text{heterogeneous loss} \qquad (5)$$

$$HCO + O_2 \rightarrow CO + HO_2 \qquad (6)$$

$$HCO \rightarrow \text{heterogeneous loss} \qquad (7)$$

In all these experiments the concentration of the stable reactants was in large excess over those of the free-radical reactant and the labile intermediates.

Under the experimental conditions described above, the ion signal intensity of HCO^+ is given by

$$I(HCO^+) = I(HCO^+)_0[k'/(k' - k'')][\exp(-k't) - \exp(-k''t)] \qquad (A)$$

where $k' = k[O_2] + k_5$ and $k'' = k_6[O_2] + k_7$.[30] k' is the first-order rate constant for C_2H_3 decay, and k is the overall rate constant of the $C_2H_3 + O_2$ reaction. A nonlinear least-squares procedure was used to obtain the values of the scaling constant $I(HCO^+)_0$ and k'' (the combined first-order rate constant for HCO loss) that give the best simulation of the measured HCO^+ ion signal profile using eq A. In the fitting procedure, k' was fixed at the value of the C_2H_3 decay rate constant (261 s^{-1} in the set of experiments performed at 599 K shown in Figure 2). The agreement between the data and the fitted curve is very good (see Figure 2). The rising portion of this fitted curve is determined largely by the measured C_2H_3 decay constant k' and to a far lesser degree by the fitting parameters $I(HCO^+)_0$ and k''.[31]

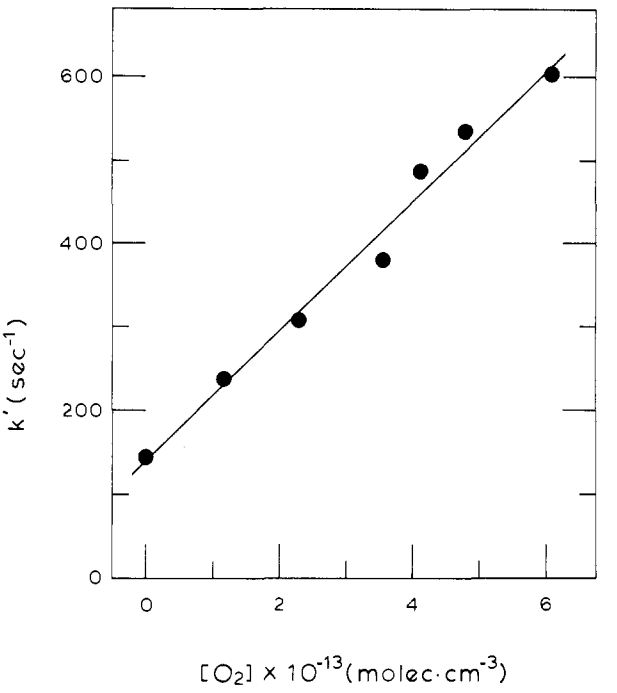

Figure 3. Plot of first-order rate constants vs. $[O_2]$ from the set of experiments conducted at 3.58 torr total pressure (primarily He) at 599 K. For conditions see Table I.

The values of k'' determined at the two temperatures at which the mechanism of the $C_2H_3 + O_2$ was studied were 332 s^{-1} at 297 K and 237 s^{-1} at 599 K. These composite rate constants for the two HCO-consuming reactions cannot be quantitatively compared with expected values since k_7, the HCO wall-loss rate constant, could not be independently measured. However, estimates of k'' can be determined. If it is presumed that $k_7 = 190$ s^{-1} at both temperatures (a wall rate constant nearly the same as those measured for the C_2H_3 radical) and that $k_6 = 5 \times 10^{-12}$ cm^3 $molecule^{-1}$ s^{-1} independent of temperature (as suggested in a recent data evaluation[7]), then the calculated values of k'' are 308 s^{-1} at 297 K and 261 s^{-1} at 599 K. Both of these calculated values are close to those obtained from the data-fitting exercise, which indicates at least semiquantitative agreement between the expected and observed rates of the HCO-consuming reactions.

The H_2CO^+ ion signal intensity is given by

$$I(H_2CO^+) = I(H_2CO^+)_0[1 - \exp(-k't)] \qquad (B)$$

Both the scaling constant ($I(H_2CO^+)_0$) and the H_2CO^+ growth constant (k') in equation B were obtained by same least-squares procedure to obtain the best agreement between this equation and the data.[30] This second fitted curve is also shown in Figure 2 together with the H_2CO^+ data. The growth constant k' for H_2CO formation obtained by the fitting procedure (264 s^{-1}) is essentially identical with the value of k' that was measured for the C_2H_3 decay, an agreement that is expected if H_2CO is an initial product of the $C_2H_3 + O_2$ reaction.

III. Rate Constant of the $C_2H_3 + O_2$ Reaction. Experiments were performed to measure the $C_2H_3 + O_2$ rate constant at four temperatures between 297 and 602 K. In addition the pressure dependence of the rate constant was studied at 363 and near 600 K. In each experiment, C_2H_3 was produced at a concentration of $\approx 1 \times 10^{11}$ molecule cm^{-3} in the presence of a large excess of O_2 (which was varied from ≈ 0.8–7×10^{13} molecule cm^{-3}). Ion signal decay profiles of $C_2H_3^+$ were always exponential in shape (see Figure 2). The monitored signals were fitted to an exponential function to obtain first-order decay constants (k'). The second-order rate constant k was obtained from the slope of the line fitted

(28) Pruss, F. J.; Slagle, I. R.; Gutman, D. *J. Phys. Chem.* **1974**, *78*, 663–665.

(29) We have recently reestablished experimentally that HCO^+ is not a fragmentation product of the photoionization of the formylmethyl radical at 10.2 eV.

(30) Prior use of this same expression is discussed in: Park, J.-Y.; Sawyer, P. F.; Heaven, M. C.; Gutman, D. *J. Phys. Chem.*, in press.

(31) Carrington, T. *Int. J. Chem. Kinet.* **1982**, *14*, 517–534.

Table I. Conditions and Results of Experiments to Measure $C_2H_3 + O_2$ Reaction Rate Constant

T, K	P, torr	10^{-16}[He], atom cm^{-3}	$10^{-13}[O_2]$, molecule cm^{-3}	$10^{12}k$,[a] cm^3 molecule^{-1} s^{-1}
297[b]	0.793	2.58	1.02–4.66	10.1
363	0.477	1.27	0.962–3.88	11.6
363	2.10	5.60	1.14–4.48	9.2
457	1.24	2.61	0.776–5.95	7.4
602	0.756	1.21	1.23–4.58	9.5
602	0.768	1.23	1.03–4.13	9.9
600	1.72	2.77	1.38–6.98	7.4
598	3.60	5.82	1.40–5.44	6.9
599	3.58	5.77	1.17–6.09	7.8

[a] Accuracy estimate: ±20%. [b] Additional experiments done at ambient temperature are reported in ref 25. $[C_2H_3Br] \approx 9 \times 10^{11}$ molecule cm^{-3} in all experiments.

through these first-order decay constants when plotted vs. $[O_2]$.[26,27] The plot of the results of the experiments conducted at 3.6 torr at 599 K is shown in Figure 3.

The conditions and results of each set of the experiments conducted to measure k are given in Table I. The estimated accuracy limits of k are ±20%. These limits are determined primarily by how well the concentrations of gases in the tubular reactor and the total pressure near the sampling point can be established. The upper temperature limit of this study was determined by the onset of increasingly variable wall conditions in the reactor that affected heterogeneous C_2H_3 loss as the temperature was increased above 600 K.

IV. Rate Constants of the $C_2H_3 + i\text{-}C_4H_{10}$ and $C_3H_5 + O_2$ Reactions. Experiments were also conducted to measure the rate constants of an H-atom abstraction reaction involving the vinyl radical and to determine whether the allyl radical reaction with O_2 proceeds by a route analogous to that observed for the $C_2H_3 + O_2$ reaction at very high temperatures. (Near ambient temperature, the $C_3H_5 + O_2$ reaction proceeds by a reversible addition mechanism.[32,33]) In both cases no reaction was observed. An upper limit of 5×10^{-14} cm^3 molecule^{-1} s^{-1} was established for both the $C_2H_3 + i\text{-}C_4H_{10}$ rate constant (at 600 K) and the $C_3H_5 + O_2$ reaction (at 900 K).[34]

Discussion

I. Products of the $C_2H_3 + O_2$ Reaction. The direct observation of HCO and H_2CO production during the $C_2H_3 + O_2$ reaction establishes reaction 2 as a major route over the temperature range of this study. Both product ion signal profiles were observed to have the temporal behavior expected from initial products. The failure to detect significant ion signals from other possible reaction products indicates that this reactive route is probably the only important one. In particular, since no C_2H_2 was observed to be formed during this reaction, the route leading to this product, reaction 1, is not a significant one up to 600 K.

The prior indirect study of the mechanism of this reaction at 753 K by Baldwin and Walker reported the same conclusion regarding the products of this reaction.[4]

II. Rate Constant of the $C_2H_3 + O_2$ Reaction. The overall rate constant of the $C_2H_3 + O_2$ reaction was found to be independent of pressure over the temperature range of this study (varying less than 20% with a 5-fold change in pressure).[25]

There is a very minor decrease in k with increasing temperature which corresponds to a negative activation energy of ≈250 cal.

$$k = 6.6\ (\pm 1.3) \times 10^{-12} \exp(250 \pm 100\ \text{cal}/RT)\ \text{cm}^3\ \text{molecule}^{-1}\ \text{s}^{-1}$$

III. Mechanism of the $C_2H_3 + O_2$ and $C_3H_5 + O_2$ Reactions. The magnitude of k, its pressure independence, and its slight decrease with increasing temperature as well as the identity of the initial products are all consistent with an addition reaction mechanism for the $C_2H_3 + O_2$ reaction at the high pressure limit. A comparable addition reaction of an alkyl radical with O_2 ($C_2H_5 + O_2$) has a similar high-pressure-limit rate constant (≈4.4×10^{-12} cm^3 molecule^{-1} s^{-1} at 295 K) but is in the middle of the pressure falloff region at the pressures of our study, 0.4–4 torr.[35] The pressure independence of k strongly suggests that the addition complex formed in the $C_2H_3 + O_2$ reaction has an extremely short lifetime, decomposing preferentially by the channel leading to the observed products rather than by redissociatioin to the original reactants.

A likely mechanism of this reaction has been suggested by Baldwin and Walker.[4]

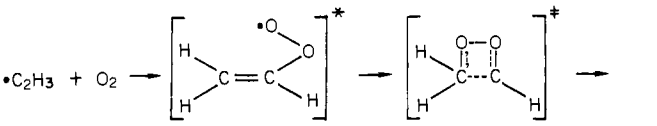

$H_2CO + \dot{H}CO$ (8)

Recently Laufer and Lechleider observed very similar behavior in the reaction of C_2H with O_2.[19] The reaction yields primarily HCO and CO (products that are analogous to those observed in the $C_2H_3 + O_2$ reaction). The rate constant at ambient temperature has a similar magnitude ($4–5 \times 10^{-12}$ cm^3 molecule^{-1} s^{-1}) as that of the $C_2H_3 + O_2$ reaction and is also pressure independent. A mechanism for the $C_2H + O_2$ reaction comparable to that shown above would also account for these results.

The different behavior of the $C_3H_5 + O_2$ reaction, i.e., reversible addition at low temperatures[32,33] (<500 K) and no rapid reaction via a route comparable to reaction 8 at higher temperatures (up to 900 K), at first appears incongruous. It can be understood, however, by using the same kind of potential energy surface that can account for the reactive pathways of the reactions of the two other unsaturated radicals (C_2H_3 and C_2H) with O_2. The ring-closing step of the mechanism shown in reaction 8 must have an energy barrier, one that may be near the strain energy of the four-membered dioxetane ring (≈ 24 kcal/mol).[36] Because of the resonance stabilization of the C_3H_5 radical, the C–O bond energy in the C_3H_5·O_2 adduct is ≈11 kcal/mol less than in the R·O_2 adducts formed with radicals that have no such stabilization (17 kcal/mol instead of 28 kcal/mol).[24,32,33] This difference places the energy barrier to ring closing in the $C_3H_5 + O_2$ reaction at or above the barrier to redissociation, while in the $C_2H_3 + O_2$ reaction this is not the case (see Figure 4). If the energy barrier along the path to ring closing is comparable to or greater than along the path to redissociation, the R·O_2 adduct will preferentially return to reactants due to the much higher entropy of activation for bond cleavage compared to ring closure.[24] This is the likely situation in the $C_3H_5 + O_2$ reaction. However, if the ring-closing barrier is 8 kcal/mol or more below the barrier to redissociation, ring closing will become the preferred pathway.

The closed-ring structures of these adducts may not actually be bound since dioxetanyl radicals have open-ring valence isomers (with no O–O bond) that are far more stable than those involving four-membered rings. It is therefore possible that the maximum potential energy along the path to ring closure corresponds to a configuration with a slightly open structure and that the barrier height is less than the ring strain energy (15–20 kcal/mol). If this is indeed the case, the relevant reactive pathways open to the C_2H_3·O_2 and C_3H_5·O_2 adducts would have the appropriate potential energy differences needed to account for the contrasting kinetics behaviors of these two R + O_2 reactions involving alkenyl radicals.

IV. Implications of these Results to Combustion Modeling. During the combustion of hydrocarbon fuels, large hydrocarbon molecules and complex free-radical intermediates rapidly either

(32) Ruiz, R. P.; Bayes, K. D.; Macpherson, M. T.; Pilling, M. J. *J. Phys. Chem.* **1981**, *85*, 1622–1624.
(33) Morgan, C. A.; Pilling, M. J.; Tulloch, J. M. *J. Chem. Soc., Faraday Trans. 2* **1982**, *78*, 1323–1330.
(34) Allyl bromide was used as the C_3H_5 precursor in these experiments.
(35) Plumb, I. C.; Ryan, K. R. *Int. J. Chem. Kinet.* **1981**, *13*, 1011–1028.
(36) Harding, L. B.; Goodard, W. A., III. *J. Am. Chem. Soc.* **1977**, *99*, 4520–4523.

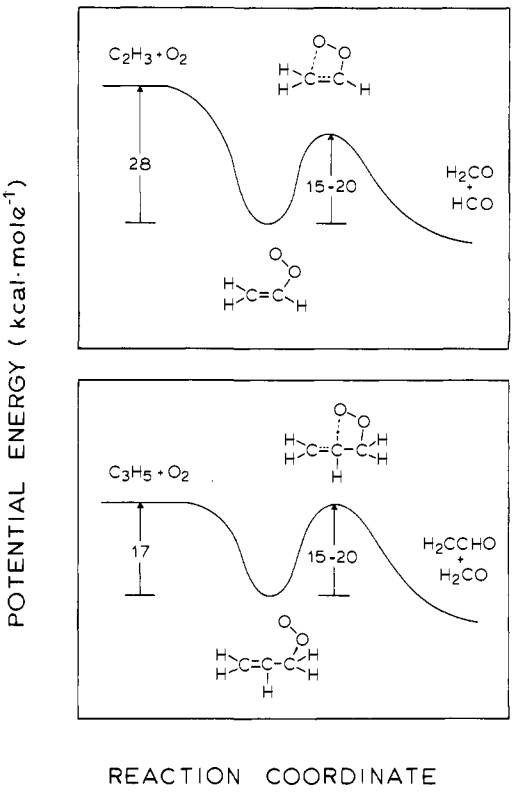

Figure 4. Qualitative potential-energy diagrams for the reaction coordinates of the $C_2H_3 + O_2$ and $C_3H_5 + O_2$ reactions.

degrade by pyrolysis and by reactions with atoms and free radicals, or oxidize and eventually form stable products including CO and CO_2.[1-10] The degradation process results in the formation of a few relatively stable alkenes and alkynes (e.g., C_2H_4 and C_2H_2) as well as carbon-rich intermediates like C_2H_3. Further loss of hydrogen atoms produces species that may polymerize to form soot. In the case of the vinyl radical, two major reactive pathways at high temperatures are

$$C_2H_3 + M \rightarrow C_2H_2 + H \quad (9)$$

$$C_2H_3 + O_2 \rightarrow HCO + H_2CO \quad (2)$$

Prior presumptions that the $C_2H_3 + O_2$ reaction yielded $C_2H_2 + HO_2$ led to conclusions that C_2H_3 primarily degrades into C_2H_2 irrespective of the reaction it undergoes. If the kinetic and mechanistic information obtained in this study can be extrapolated to still higher temperatures, then reaction 2 provides a distinctly different fate for the carbon contained in the vinyl radicals under combustion conditions. Using our expression for k (and presuming there is no mechanism change above 600 K) and a literature value for k_9 (1.3×10^{-9} exp(-31.5 kcal mol$^{-1}/RT$) cm^3 molecule^{-1} s^{-1}),[13] one can calculate that in air ($[M]/[O_2] = 5$) the oxidation of vinyl radical will be the more prominent of the two routes (reactions 2 and 9) up to 2000 °C. Thus, in most combustion processes, particularly those run under lean conditions, reaction 2 will be an important elementary reaction.

Additional studies of the kinetics and mechanism of the reactions of unsaturated hydrocarbon free radicals with molecular oxygen are in progress.

Acknowledgment. This research was supported by the Department of Energy under Contract No. DE-AC02-78ER14593. We thank Dr. Lawrence B. Harding, Chemistry Division, Argonne National Laboratory, for useful discussions regarding the mechanisms of the reactions studied and Paul F. Sawyer for his development of the computer codes that were used to obtain and process kinetic data. We also gratefully acknowledge the Research corporation for the award of a Cottrell Research Grant (9899) which provided the excimer laser used in this study.

Registry No. C_2H_3Br, 593-60-2; i-C_4H_{10}, 75-28-5; O_2, 7782-44-7; vinyl radical, 2669-89-8; allyl radical, 1981-80-2.